

Delft

NAVAL SHIP RESEARCH AND DEVELOPMENT CENTER

Washington, D.C. 20007



DEVELOPMENT OF A HYDROFOIL WATERJET
PROPULSION SYSTEM TEST FACILITY

by

T.T. Huang and G.S. Belt

This document has been approved for
public release and sale; its distri-
bution is unlimited.

DEPARTMENT OF HYDROMECHANICS
RESEARCH AND DEVELOPMENT REPORT

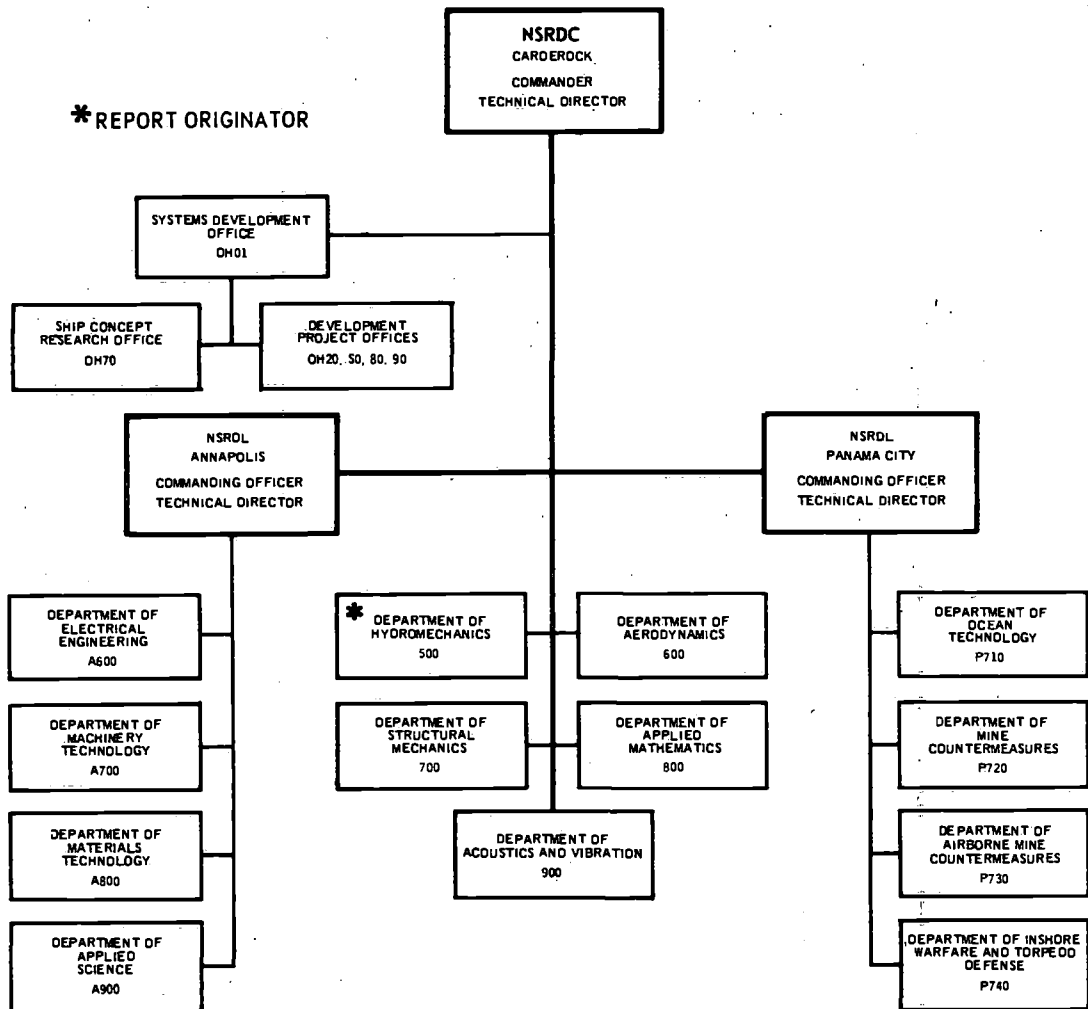
May 1970

Report 3318

The Naval Ship Research and Development Center is a U.S. Navy center for laboratory effort directed at achieving improved sea and air vehicles. It was formed in March 1967 by merging the David Taylor Model Basin at Carderock, Maryland and the Marine Engineering Laboratory (now Naval Ship R & D Laboratory) at Annapolis, Maryland. The Mine Defense Laboratory (now Naval Ship R & D Laboratory) Panama City, Florida became part of the Center in November 1967.

Naval Ship Research and Development Center
Washington, D.C. 20007

MAJOR NSRDC ORGANIZATIONAL COMPONENTS



DEPARTMENT OF THE NAVY
NAVAL SHIP RESEARCH AND DEVELOPMENT CENTER
WASHINGTON, D. C. 20007

DEVELOPMENT OF A HYDROFOIL WATERJET
PROPULSION SYSTEM TEST FACILITY

by

T.T. Huang and G.S. Belt

This document has been approved for
public release and sale; its distri-
bution is unlimited.

May 1970

Report 3318

TABLE OF CONTENTS

| | Page |
|--------------------------------------|------|
| ABSTRACT | 1 |
| ADMINISTRATIVE INFORMATION | 1 |
| INTRODUCTION | 1 |
| MODEL SCALING LAWS | 2 |
| FACILITY, APPARATUS, AND MODEL | 3 |
| FACILITY | 3 |
| APPARATUS | 4 |
| MODEL | 8 |
| TEST PROCEDURE AND ACCURACY | 8 |
| REDUCTION OF DATA | 15 |
| RESULTS AND DISCUSSION | 16 |
| CONCLUSIONS | 23 |
| RECOMMENDATIONS | 23 |
| REFERENCES | 25 |

LIST OF FIGURES

| | Page |
|---|------|
| Figure 1 - Hydrofoil Waterjet Propulsion Test Rig | 5 |
| Figure 2 - Sketch of Hydrofoil Waterjet Test Rig | 6 |
| Figure 3 - Gage Assembly | 7 |
| Figure 4 - Hydrofoil Model | 9 |
| Figure 5 - Details of the Model | 10 |
| Figure 6 - Locations of Pressure Taps and Total Head Tubes on the Model | 11 |
| Figure 7 - Sketch of Force Measurements with the Presence of Flexible Joint | 13 |
| Figure 8 - Comparative Results for Lift and Drag at Takeoff | 17 |
| Figure 9 - Comparative Results for Lift and Drag at Cruise | 18 |
| Figure 10 - Effect of Inlet Velocity on the External Nacelle Pressure Distribution at Design Cruise Speed of 50 Knots | 20 |
| Figure 11 - Effect of Submergence on the External Pressure Distribution at Cruise | 21 |
| Figure 12 - Effect of Yaw Angle and Submergence on the External Peripheral Pressure Distribution at Cruise | 22 |
| Figure 13 - Head Loss Coefficients from Inlet to Strut Exit | 24 |

NOTATION

| | |
|-------|---|
| A_j | Internal cross-sectional area of the flexible rubber joint, sq ft |
| C_D | Drag coefficient, $\frac{D}{\frac{1}{2} \rho V_o^2 S}$ |
| C_L | Lift coefficient, $\frac{L}{\frac{1}{2} \rho V_o^2 S}$ |
| C_p | Pressure coefficient, $\frac{p - p_o}{\frac{1}{2} \rho V_o^2}$ |
| D | Drag of the model, lbs |
| D_g | Drag sensed by the gage, assembly, lbs |
| D_j | Drag transmitted through the flexible joint, lbs |
| D_M | The momentum of the entering fluid at inlet, lbs |
| F_n | Froude number, V/\sqrt{gh} |
| g | Gravitational acceleration, ft/sec ² |
| H_D | Head loss from inlet to strut exit, ft |
| h | Submergence of the nacelle centerline, ft |
| L | Lift of the model, lbs |
| L_g | Lift sensed by the gage assembly, lbs |
| L_j | Lift transmitted through the flexible joint, lbs |
| L_M | The momentum of the leaving fluid at strut exit, lbs |
| P | Local pressure, lb/sq ft |
| P_j | Internal pressure at the flexible joint, lb/sq ft |
| p_o | Ambient pressure, lb/sq ft |
| P_v | Vapor pressure of water, lb/sq ft |
| R_I | Inlet Reynolds number, $\frac{R_i V_i}{\nu}$ |
| R_i | Radius of inlet, ft |
| S | Total plane area of the foil, sq ft |

- V_e Average velocity at the strut exit, ft/sec
 V_i Velocity at inlet, ft/sec
 V_o Freestream velocity, ft/sec
 θ Angle between vertical line and static pressure tap on the nacelle, deg
 ν Kinematic viscosity of water, ft²/sec
 ρ Mass density of water, lb-sec²/ft⁴
 σ Freestream cavitation number, $\frac{P_o - P_v}{\frac{1}{2} \rho V_o^2}$
 ψ Yaw angle, deg

ABSTRACT

The Naval Ship Research and Development Center (NSRDC) has established the capability for conducting hydrofoil waterjet propulsion tests. A test rig was designed and built, utilizing an existing planar-motion mechanism (PMM), for use in the high-speed towing basin. An experimental procedure and associated instrumentation were also developed for these experiments. An experiment using an existing nacelle-strut-foil hydrofoil model was made to demonstrate this capability at the Center.

ADMINISTRATIVE INFORMATION

This work was supported by the Hydrofoil Development Program Office under Task No. 01722, NSRDC Problem No. 526-188.

INTRODUCTION

A waterjet propulsion system can be attractive for propelling high-speed marine vehicles such as hydrofoil craft. The advantages offered by such a system are elimination of complex transmission machinery and possible reduction of underwater radiated noise.

A satisfactory waterjet propulsion system should possess a cavitation-free inlet, an efficient ducting system, and a lightweight pump capable of sustaining high performance with nonuniform inflow and with some blade cavitation. Only limited theoretical design methods exist for these critical waterjet components, and the final practical design still depends on experimental data. Furthermore, the mutual interference between system components and the performance of a complete waterjet system are, at present, beyond the scope of theoretical evaluation. Therefore, reliable experimental techniques for predicting the performance of waterjet components and of the complete system are essential for the design of optimized waterjet propulsion systems.

NSRDC has carried out a program to develop experimental techniques for evaluating waterjet components as well as a complete waterjet propulsion system. The investigation reported herein is part of this program. The primary purpose of this work is to design, build, and demonstrate a waterjet propulsion test rig suitable for high-speed waterjet experiments. A test rig, modified from an existing planar-motion

mechanism has been developed. The rig can be towed by Carriage 5 of the high-speed basin at NSRDC. The test rig is capable of measuring static force components experienced by the model with the waterjet inlet operating. Control for varying angle of attack, yaw angle, and depth of the model is available.

The developed test rig was used to perform a test on an existing scaled hydrofoil model of nacelle-strut-foil configuration designed and tested previously by Lockheed California Company.¹ The model was tested at Froude-scaled values of the prototype takeoff and cruise speeds. The test program covered adequate ranges of inlet velocity ratio V_i/V_o . Submergence h , and yaw angle ψ , for direct comparison with the Lockheed results.

A detailed description of the associated facilities, instrumentation, and testing techniques employed in the investigation is also given in this report.

MODEL SCALING LAWS

The purposes of conducting model tests on a hydrofoil nacelle-strut-foil configuration were:

1. To predict or verify the estimated lift-drag performance of a complete hydrofoil nacelle-strut-foil system. The essential conditions are cruise speed, hump speed, and rough-water performance which may be estimated from off-design performance tests (varying yaw and angle of attack from the design values).

2. To study the mutual hydrodynamic interference among the individual components. The important factors are free-surface effects on nacelle pressure distribution, effect of strut and foil on nacelle performance, and effect of inlet velocity ratio on foil performance.

3. To investigate the cavitation characteristics of a nacelle. The critical areas are external nacelle cavitation at cruise, internal nacelle cavitation at hump, and effects of free surface and waves on nacelle cavitation characteristics.

¹References are listed on page 25.

4. To provide hydrodynamic information for the design and selection of a pump, i.e., duct loss and inflow velocity distribution to the pump.

The model must not only be to geometric scale in all respects, but must also be tested under conditions which comply as nearly as possible with the laws of dynamic similitude. To satisfy Items 1 through 4 requires maintaining similarity in terms of Froude number, cavitation number, and Reynolds number simultaneously, which is not possible except by going to a costly full-scale model. However, if the prime dynamic similarity law can be maintained and the effects of the secondary similarity laws can be estimated, then the smaller scale model is valuable.

The following procedure was developed at NSRDC for the hydrofoil waterjet test:

(a) Items 1 and 2 were studied by means of Froude scaling laws. The prediction of full-scale drag should be subject to the Reynolds scaling law and the ITTC skin friction line may be used.

(b) For Item 3 the pressure distribution on the critical area(s) of the nacelle was measured. Froude scaling law should be used for the pressure measurement. However, for deep submergence and high Froude number, the pressure coefficient measurement may be independent of Froude number, and the model can be tested at the corresponding cavitation numbers of the full-scale craft. The actual cavitation inception on the nacelle can be studied by observation.

(c) For Item 4 the Reynolds scaling law was more important than the Froude scaling law. However, it is usually impossible to attain the full-scale Reynolds numbers in model tests and attempts should be made to increase the Reynolds number of the flow through the model duct to as high a value as possible. The full-scale duct loss coefficient may be extrapolated from a plot of loss coefficient versus Reynolds number.

FACILITY, APPARATUS, AND MODEL

FACILITY

The facility used for this study was the high-speed basin at NSRDC.² The high-speed basin is 2968 ft long, 21 ft wide, 10 ft deep for one-third of its length, and 16 ft deep for the remaining length. A

pneumatic wavemaker is also installed in this facility to permit the generation of waves of uniform length and height. Carriage 5 can be operated at speeds up to 60 knots. The advantages of using the high-speed basin for the high-speed waterjet propulsion tests are: (1) long constant velocity run, (2) high-speed capability up to 60 knots, (3) sufficient electrical power available for operating large pumps, and (4) option for studying the effect of waves.

APPARATUS

The test rig modified from an existing planar-motion mechanism is shown in Figures 1 and 2. A 185-horsepower pump manufactured by Curtiss-Wright Corporation (Model M-185) was used in the test. The pump was driven by a 200-horsepower motor. In operation, water flows into the nacelle inlet, up the strut, and through a flexible rubber joint. From this point, the water passes into the pump and through a 6-in. pipe. The pipe straightens the flow before it enters the nozzle where the discharge is measured. At the end, an elbow deflects the flow back to the basin.

The PMM Penthouse facility, with electronic depth and pitch controls, was originally made for stability and control model tests. The towing apparatus with mechanical yaw control was designed and manufactured for the present work.

The gage system and associated recording equipment are shown in Figure 3. It is essentially the same as that used in the basic NSRDC hydrofoil lift-drag experimental rig.³ Three gage assemblies were mounted between the two ends of the flexible rubber joint which allowed the flow to pass through and transmit negligible load. Each gage assembly consisted of two modular force gages connected in series and oriented to measure vertical and horizontal forces, together with either a single- or double-hinged pivot. The hinged pivots permitted movement to eliminate all misalignment and unwanted moments about their own individual axis. However, collectively, they provided restraint to all the motions of the model. The flexible rubber joint, whose stiffness varied slightly with pressure in the internal duct system, necessitated calibrations to obtain appropriate corrections for the lift and drag forces. The outputs of the force gages were displayed on a digital recording system. The shaft rpm of the motor was sensed and read out by a magnetic pickup and frequency counter.

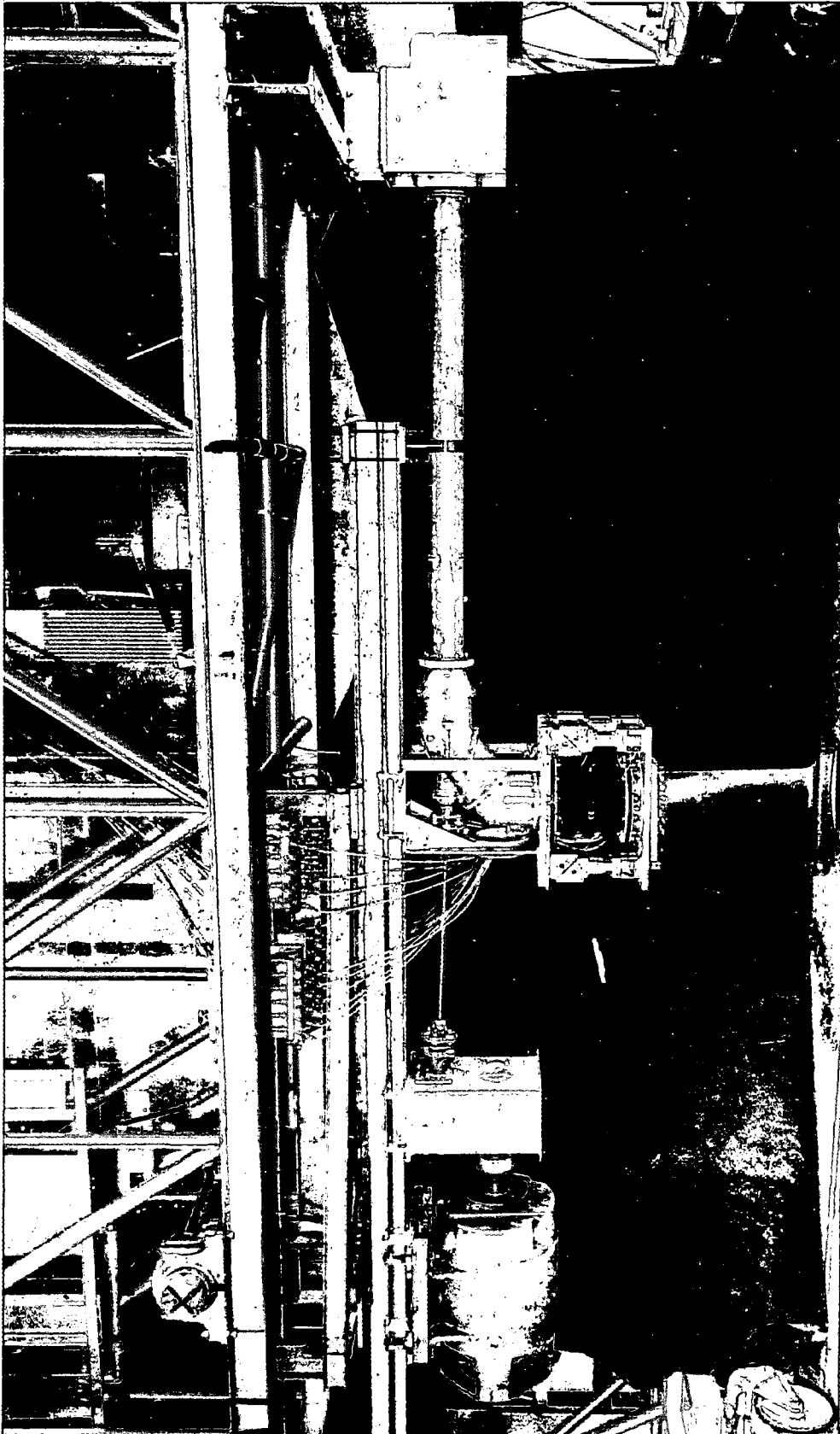


Figure 1 - Hydrofoil Waterjet Propulsion Test Rig

| Number | Description | Quantity | Number | Description | Quantity | Number | Description | Quantity |
|--------|------------------------|----------|--------|--|----------|--------|---------------------------|----------|
| 1 | Pivot Beam | 1 | 15 | Motor Base Plate | 2 | 29 | Orifice | 1 |
| 2 | Pivot Beam Stub Shaft | 2 | 16 | Motor Base Plate Clamp | 4 | 30 | Cast Fairing | 2 |
| 3 | Tilt Beam | 1 | 17 | Gear Box | 1 | 31 | Pump Mount Assembly Clamp | 1 |
| 4 | Guide Roller Assembly | 2 | 18 | Gear Box Base Plate Clamp | 2 | 32 | Pump Mount Assembly | 1 |
| 5 | Tilt Half Pivot (Male) | 1 | 19 | 200-HP motor Base | 1 | 33 | Adapter Plate | 1 |
| 6 | Block Support | 3 | 20 | Coupling | 1 | 34 | Flanged Duct | 1 |
| 7 | Yaw Beam | 1 | 21 | Universal Shaft | 1 | 35 | Flexible Joint | 1 |
| 8 | Clamp | 4 | 22 | Universal Shaft | 1 | 36 | Gage Mount | 1 |
| 9 | Cam Rollers | 3 | 23 | Universal Shaft | 1 | 37 | Hydrofoil Adapter Plate | 1 |
| 10 | Clamp Base | 1 | 24 | M185 Pump | 1 | 38 | Hydrofoil (male) | 1 |
| 11 | Planar Motion Beam | 1 | 25 | Nozzle | 1 | 39 | Block Gage Bracket | 6 |
| 12 | Washer | 1 | 26 | Flexible Joint | 1 | 40 | Block Gage 4" x 4" x 4" | 2 |
| 13 | Lock Nut | 1 | 27 | Butterfly Valve with Pneumatic Control | 1 | 41 | Double Pivot | 2 |
| 14 | Stud Plate | 1 | 28 | Ducting | 1 | 42 | Single Pivot | 1 |

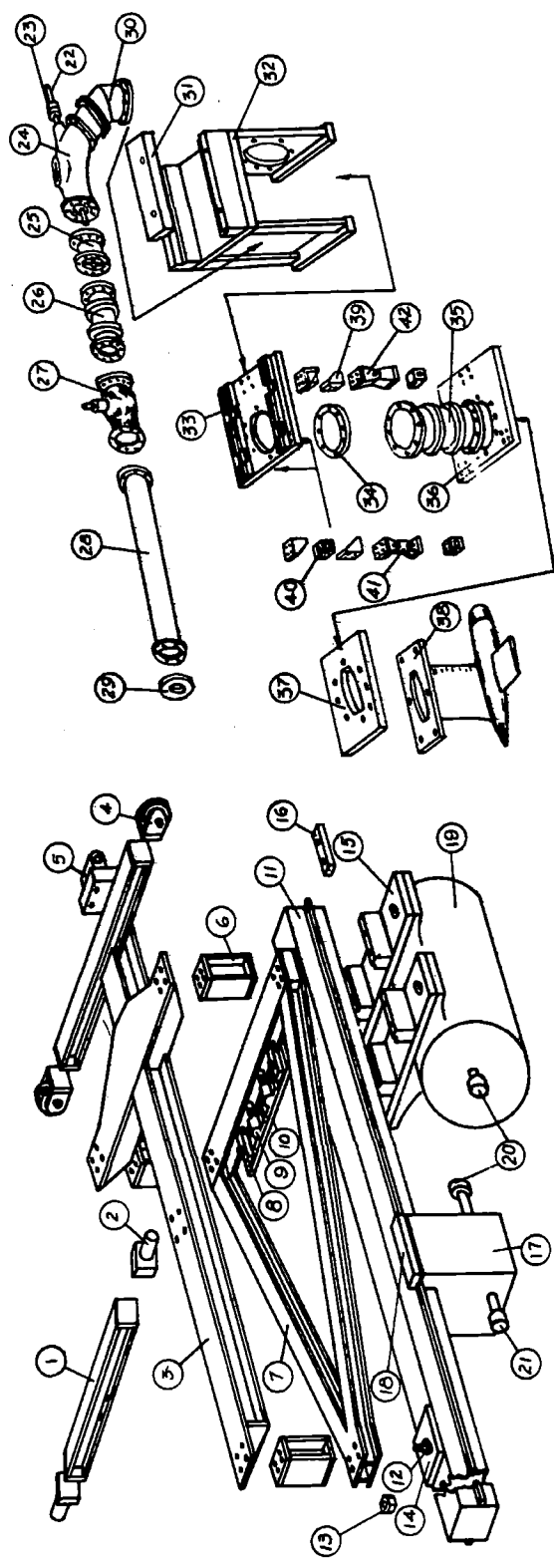


Figure 2 - Sketch of Hydrofoil Waterjet Test Rig

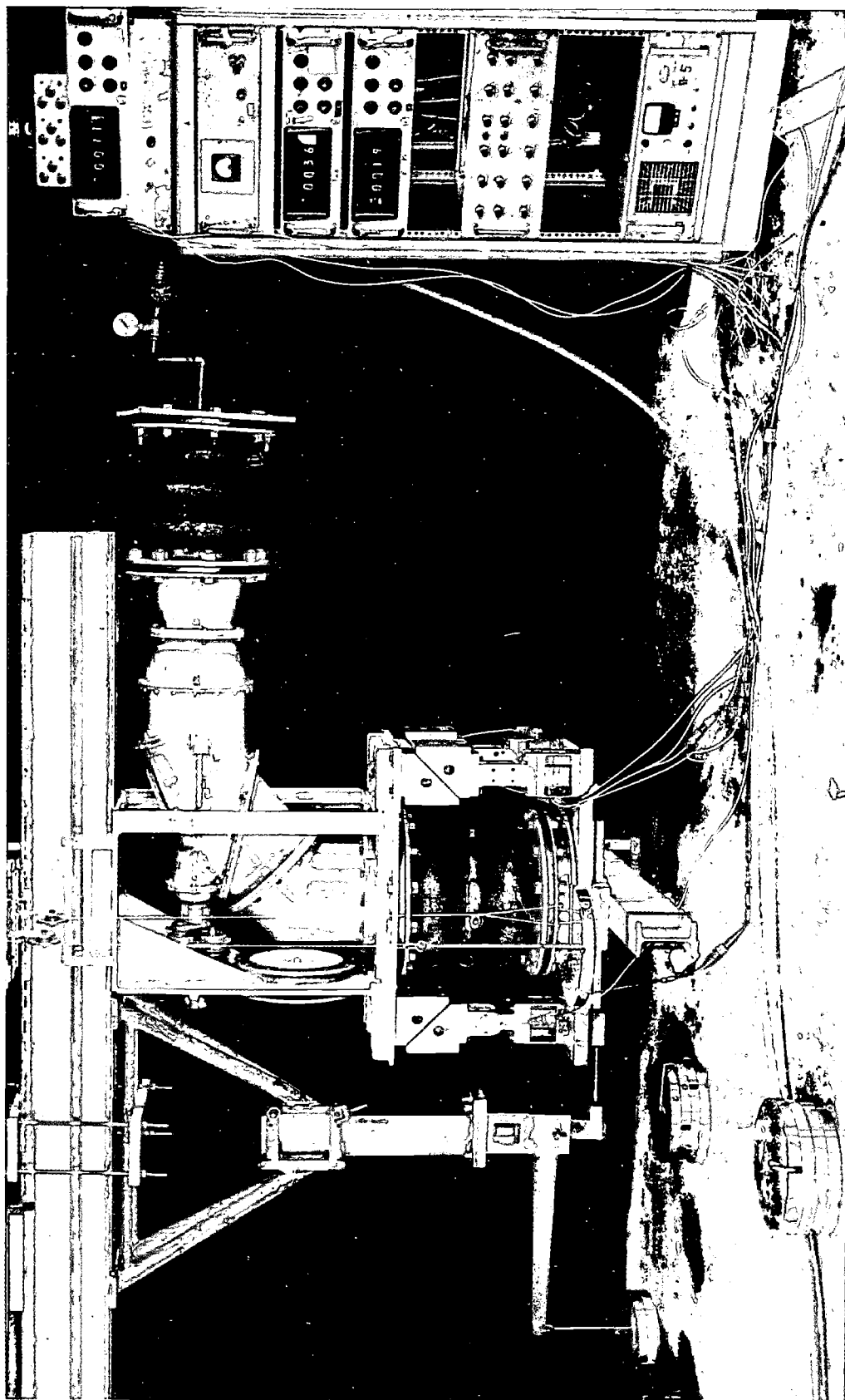


Figure 3 - Gage Assembly

All pressure measurements were taken by transducers with strain-gaged diaphragms (Dynisco PT 25-10). A digital data logging system was used to collect the large amount of the pressure measurement.

The flow rate through the waterjet system was measured by a nozzle located at the end of the 6-in. pipe. Two nozzles were used alternately to cover the large range of flow rate. One was a 2.4-in. diameter orifice⁴ and the other was a long radius nozzle⁵ of 4.2-in. diameter.

MODEL

A one-tenth linear scale model of a full-scale nacelle-strut-foil subcavitating hydrofoil configuration was used. This model, representing a waterjet propulsion intake system for a 50-knot hydrofoil boat, was designed and built by Lockheed California Company.¹ The model is shown in Figure 4 and the pertinent geometrical characteristics are shown in Figure 5 in terms of model dimensions. The flow characteristics of this model were measured by the following instrumentation:

1. Static pressure taps were distributed over the critical region of the inlet nose so that the cavitation inception could be ascertained and compared to the predicted data.

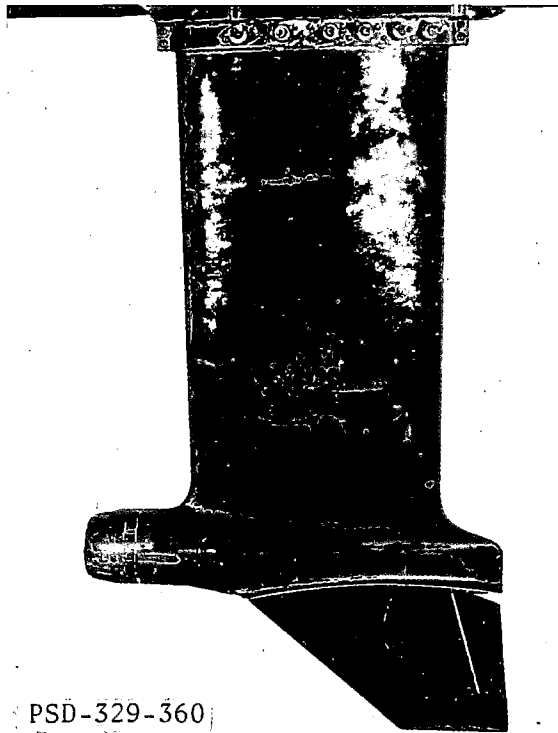
2. A total head rake was installed in the inlet to determine the magnitude of the total pressure distortion at various angles of attack and yaw.

3. Total heads were measured at the strut exit to determine the overall pressure recovery characteristics.

All pressure measurements were taken using strain-gaged transducers. The gages were located as close as possible to the pressure sampling points, and allowed all lines to lead upward to a pressure manifold which provided an air-bleeding system for all the lines. The locations of the pressure taps and total head tubes are shown in Figure 6.

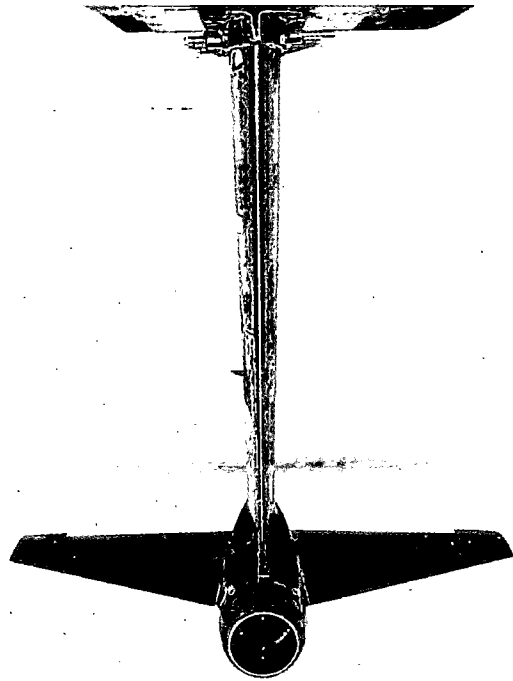
TEST PROCEDURE AND ACCURACY

Prior to conducting the test program in the high-speed basin, all the instruments were carefully calibrated. Each pressure transducer was calibrated over the anticipated range of loading by applying pressures by means of columns of water at several heights. Within the range tested,



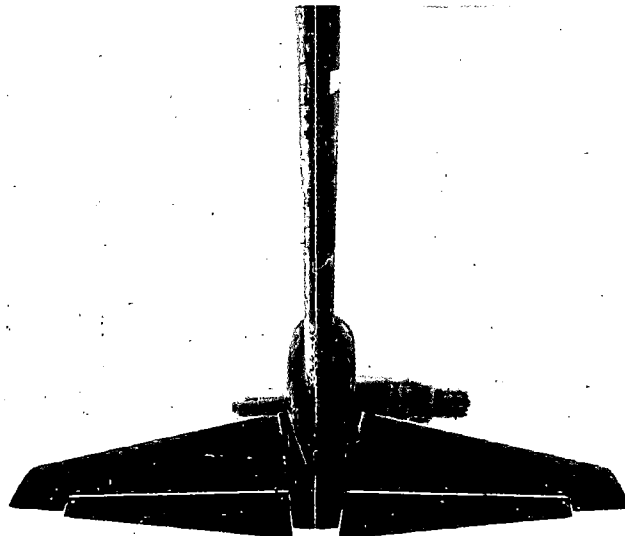
PSD-329-360

Side View



PSD-329-361

Front View



PSD-329-359

Rear View

Figure 4 - Hydrofoil Model

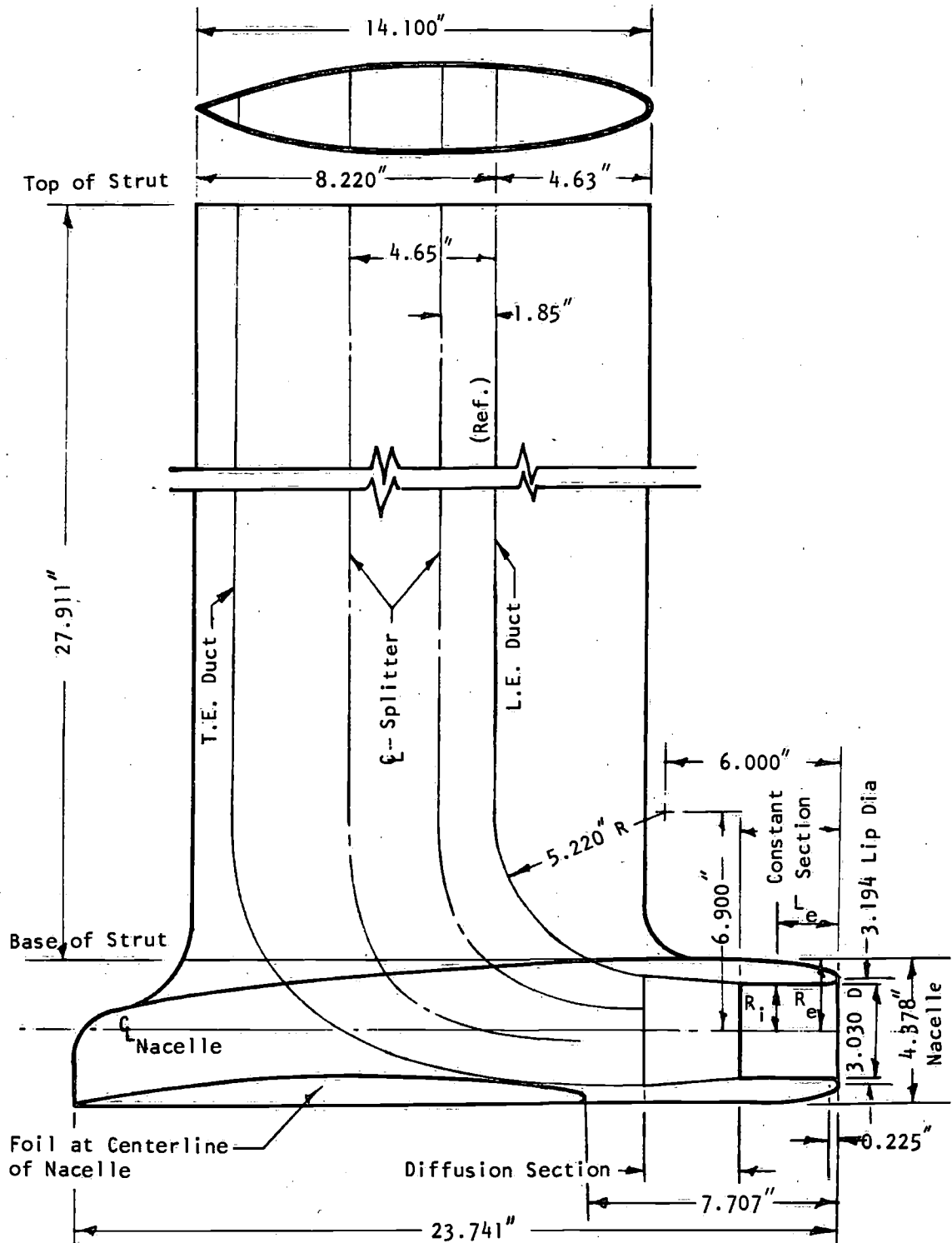


Figure 5 - Details of the Model

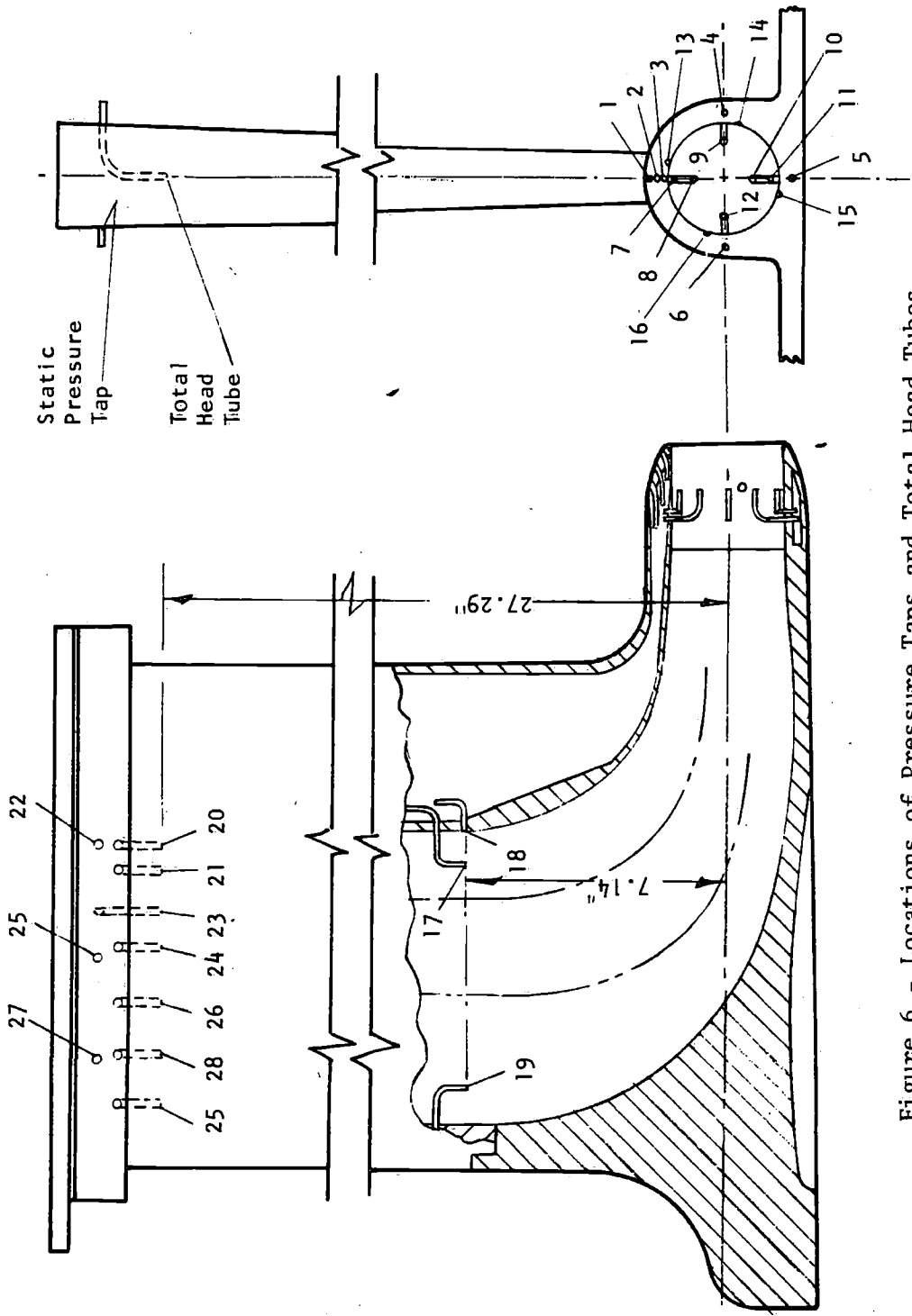


Figure 6 - Locations of Pressure Taps and Total Head Tubes on the Model

all calibration curves for the transducers were linear. The calibration of the modular force gages is very critical because of the presence of a flexible rubber joint. The flexible joint may be considered as a spring which transmits only a small part of the loading. The following procedure was used to make the appropriate corrections.

1. The modular force gages were individually calibrated with standardized weights to obtain their sensitivity factors in a controlled environment.

2. The gages were installed in a gage assembly which was connected to a top plate attached to the pump housing and to a bottom plate which was attached to the model. During this operation, the tension of the mounting bolt was carefully adjusted to ensure that the drag gage read zero and the lift gage read only a force which was compatible to the weight of the bottom plate. This served as a check to eliminate unwanted initial moments about the gage axes.

3. The internal duct system was then sealed and a pressure was applied to the duct system. The complete gage assembly was calibrated by applying known drag and lift forces as shown in Figure 3. The flexible rubber joint was considered as a spring, as shown in Figure 7. The applied lift and drag forces (L_g , D_g) were sensed mostly by the gage assembly, and a small part of the forces, i.e., L_j , D_j , was transmitted through the flexible joint. Disregarding the internal flow, the following relationships hold:

$$L - p_j A_j = L_g + L_j = \left(1 + \frac{L_j}{L_g}\right) L_g$$

and

$$D = D_g + D_j = \left(1 + \frac{D_j}{D_g}\right) D_g$$

During calibration, external lift and drag forces L and D were applied by using known weights, and forces L_g and D_g were read from the gages. $p_j A_j$ was derived from the internal pressure at the flexible joint p_j measured by a pressure transducer, and the internal cross sectional area of the flexible joint A_j . For all expected lift, drag, and internal pressure values ($p_j < 15$ psi), it was found that $L_j/L_g = 0.03$ and $D_j/D_g = 0.13$.

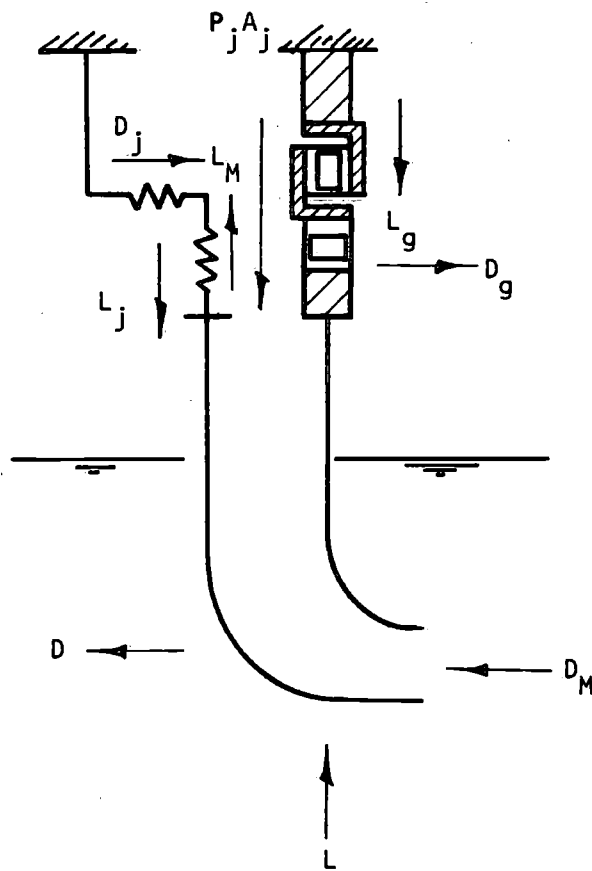


Figure 7 - Sketch of Force Measurements with the Presence of Flexible Joint

After completing all the calibrations, the test rig was attached to the towing carriage. At selected times during the tests, all the pressure lines were bled and the digital readout systems were balanced and adjusted to read zero for the modular gages and the pressure transducers. Then, for a given model setting of yaw angle, depth of submergence, and angle of attack, the model was brought up to a predetermined carriage speed corresponding to the Froude scale value of the full-scale takeoff or cruise speed. At the same time the pump rpm in the propulsion system was adjusted to a given inlet velocity which was determined from the pressure reading of the calibrated nozzles.^{4,5} When steady conditions were reached, the run was maintained for at least 20 seconds while the lift, drag, and pressure data were measured.

The test program covered the variation of the following parameters: (1) freestream velocity V_o corresponding to the prototype takeoff and cruise speeds of 30 and 50 knots, respectively; (2) inlet velocity ratio V_i/V_o from 0.75 to 1.2 for takeoff runs and V_i/V_o from 0 to 0.0 for cruise runs; (3) yaw angle ψ of 0 and 4 deg; (4) submergence h for model-scaled prototype values of 8.4 and 5.5 ft for the cruise runs, and 16.4 and 8.4 ft for the takeoff runs; and (5) no flap at cruise and ten-deg flap angle at takeoff.

No attempt was made to obtain a complete error analysis for this test. However, the test accuracy of the instrumentation can be evaluated from the calibrations of the complete system and variations of the instrument outputs during a given test.

The instrument error was estimated as follows:

- | | |
|-------------------------|-----------------|
| 1. Pressure measurement | ± 1 percent |
| 2. Force measurements | ± 3 percent |
| 3. Carriage speed | ± 0.01 fps |
| 4. Inlet velocity | ± 2 percent |
| 5. Angle of attack | ± 0.2 deg |
| 6. Submergence | ± 0.1 in. |

REDUCTION OF DATA

The methods used to reduce the data are typical of current practices followed at NSRDC in connection with captive model lift, drag, and pressure measuring techniques for hydrofoil waterjet propulsion systems. The procedural steps were as follows:

1. The lift and drag forces measured as reactions at the gage assembly by each of the six modular gages were added vectorially to obtain the total model lift and drag forces.

2. The outputs of pressure transducers were accepted by the digital logging system and were converted to pressure readings (psf) using the calibration curves. The pressure coefficients were then computed, i.e.,

$$C_p = \frac{p - p_o}{\frac{1}{2} \rho V_o^2}$$

where p is the measured local static pressure on the body,

p_o is the ambient pressure,

ρ is the mass density of the water, and

V_o is the free stream velocity.

When the local static pressure on the body is equal to the vapor pressure, then the cavitation inception is assumed to occur. Under this condition,

$$-C_p = \frac{p_o - p}{\frac{1}{2} \rho V_o^2} = \frac{p_o - p}{\frac{1}{2} \rho V_o^2} = \sigma$$

where σ is the freestream cavitation number.

3. The total forces measured by the modular gages were corrected to account for the tare of the flexible joint and the momentum of the fluid at the inlet and strut exit. As shown in Figure 7, the momentum of the entering fluid D_M was in the same direction as the model drag and since this component was included in the gage reading D_g the actual model drag D was obtained from

$$D = D_g + D_j = D_M = \left(1 + \frac{D_j}{D_g}\right) D_g - D_M$$

where D_j is the drag force transmitted by the flexible joint,

$$D_j/D_g = 0.13 \text{ (by calibration),}$$

$$D_M = \rho Q V_i = \rho \left(\frac{V_i}{V_o} \right)^2 V_o^2 A_i, \text{ and}$$

Q is measured by the nozzle.

The momentum of the fluid leaving the model, L_M , was in the direction opposite to the model lift L , and was added to the gage reading L_g to obtain the actual model lift from

$$L = p_j A_j + L_g + L_j - L_M = p_j A_j + \left(1 + \frac{L_j}{L_g} \right) L_g - L_M$$

where L_j is the lift force transmitted by the flexible joint,

$$L_j/L_g = 0.03 \text{ (by calibration),}$$

p_j is the internal pressure inside the flexible joint measured by a transducer,

A_j is the internal cross section of the joint,

$$L_M = Q V_e, \text{ and}$$

V_e is the average velocity at the strut exit (L_M is small compared with $p_j A_j$).

The corrected force coefficients were then computed, i.e.,

$$C_L = \frac{L}{\frac{1}{2} \rho V_o^2 S}, \text{ and } C_D = \frac{D}{\frac{1}{2} \rho V_o^2 S}$$

The reference area S is the total area of the foil and was 2.25 sq ft.

RESULTS AND DISCUSSION

The measured lift and drag forces at takeoff are shown in Figure 8, while Figure 9 shows the measured forces at cruise speed. The results of the present study compare well with that of Lockheed. It may be noted that the effect of inlet velocity ratio on the overall lift and drag characteristics of the hydrofoil tested is rather small. The lift-drag ratio of this model is about 9.5 at cruise speed and at takeoff speed.

Submergence ----- 8.4 ft
 Angle of Attack ----- 0
 Flap Angle ----- 10°
 Yaw Angle ----- 0°

NSRDC -----○
 Lockheed ---□

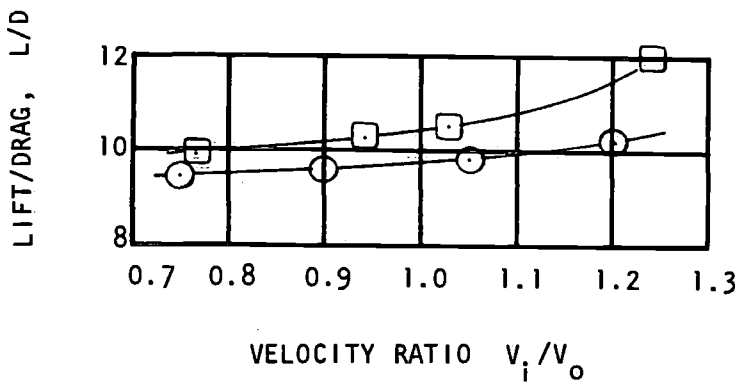
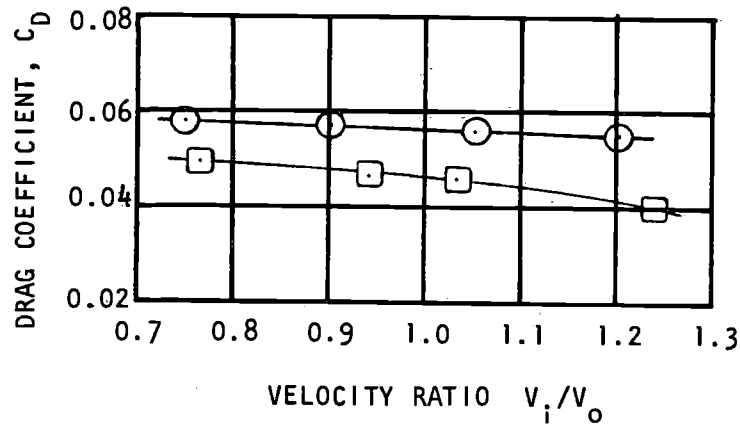
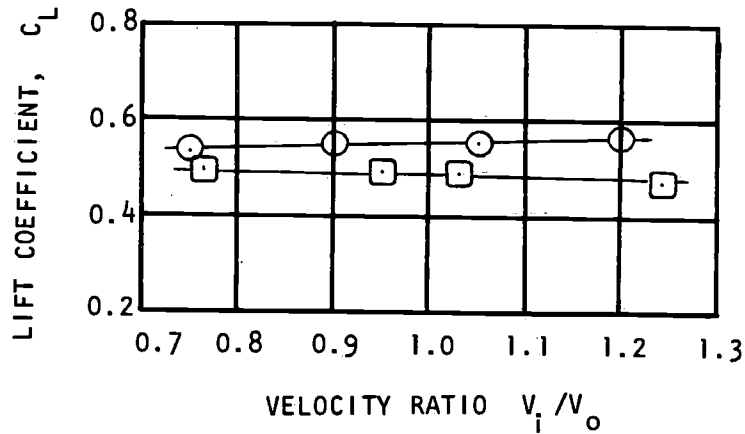


Figure 8 - Comparative Results for Lift and Drag at Takeoff

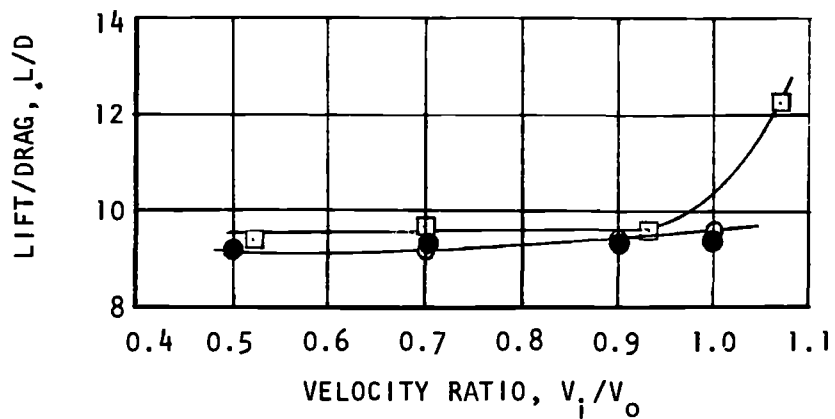
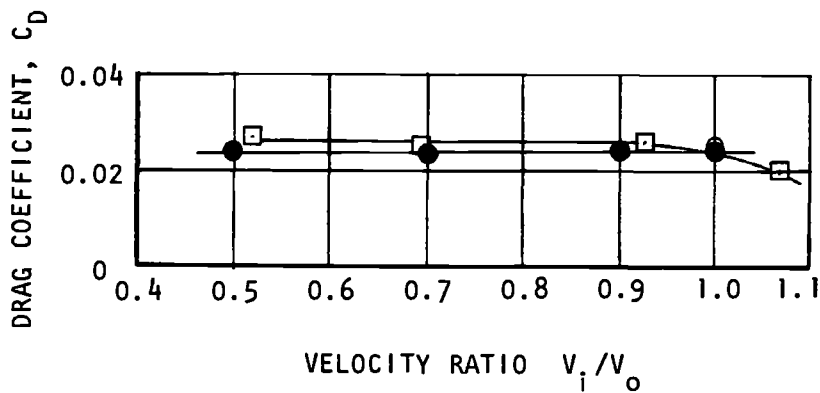
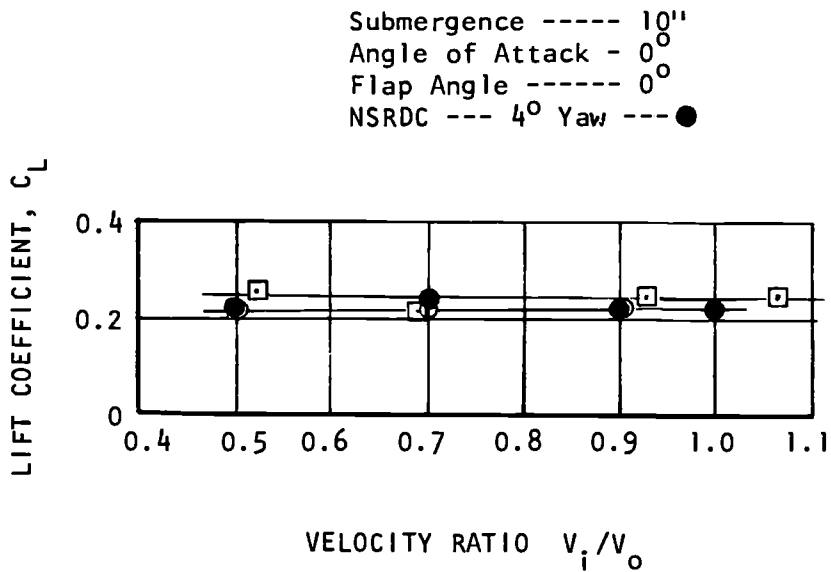


Figure 9 - Comparative Results for Lift and Drag at Cruise

The effect of inlet velocity and depth of submergence on the external nacelle pressure distribution at cruise speed is shown in Figure 10. At a cruise speed of 50 knots and a submergence of 8.4 ft, the freestream cavitation number σ is 0.37 (based on V_o). Therefore, inlet velocity ratios less than $V_i/V_o = 0.5$ are predicted to result in external cavitation. Likewise, for a submergence of 5.5 ft, i.e., $\sigma = 0.34$, inlet velocity ratios less than $V_i/V_o = 0.6$ are predicted to result in external cavitation.

Figure 11 shows a plot of pressure coefficients for the design cruise conditions ($V_i/V_o = 0.7$, $V_o = 50$ knots) and two values of submergence. As can be seen, there is a slight decrease in C_p as the submergence is decreased. It is found from Figure 11 that the nacelle is free from cavitation at design conditions. Similar trends were found at Lockheed. However, considerable discrepancy in the magnitude of the measured pressure coefficients between the NSRDC and Lockheed results is noted. The NSRDC data are considered more reliable since its facility allows longer time of constant speed for collecting the pressure data.

Yaw angles of 0 and 4 deg were tested at the cruise velocity of 50 knots and four inlet velocity ratios. Four static probes were located aft of the inlet lip on the top, bottom, port, and starboard sides of the nacelle and are defined by the angle θ , measuring clockwise looking into the inlet. Figure 12 shows the data obtained from these probes with the model yawed to the port side. The pressures on the starboard side are increased while those on the port side have decreased. It should be noted that at 4 deg yaw the nacelle cavitation should occur even at $V_i/V_o = 0.7$. Thus, nacelle cavitation may occur in rough seas when the effective yaw angle or angle of attack exceeds the design values of 4 deg.

Internal nacelle cavitation at takeoff was not predicted within the range of inlet velocity ratios tested. No further study was attempted.

The inlet velocity profile and total head profile at the strut exit were found to be quite uniform for all cases tested, and these data are not presented.

Based on the tests, the nacelle is predicted to be cavitation-free at design cruise speed of 50 knots and at design inlet velocity ratio (V_i/V_o) of 0.7. However, slight cavitation may occur for rough seas at the

$V_i/V_o = 0.9 - \circ$
 $0.7 - \square$
 $0.5 - \diamond$
 $0.3 - \triangle$
 $0.0 - \nabla$

NSRDC $\text{---} \bullet \text{---}$
 Lockheed $\text{---} \circ \text{---}$

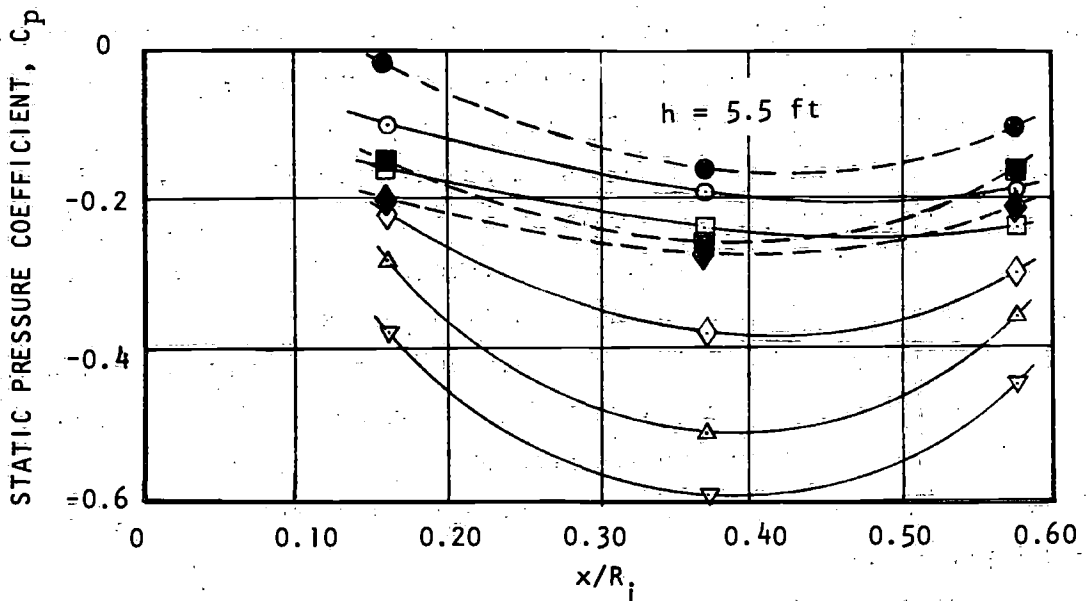
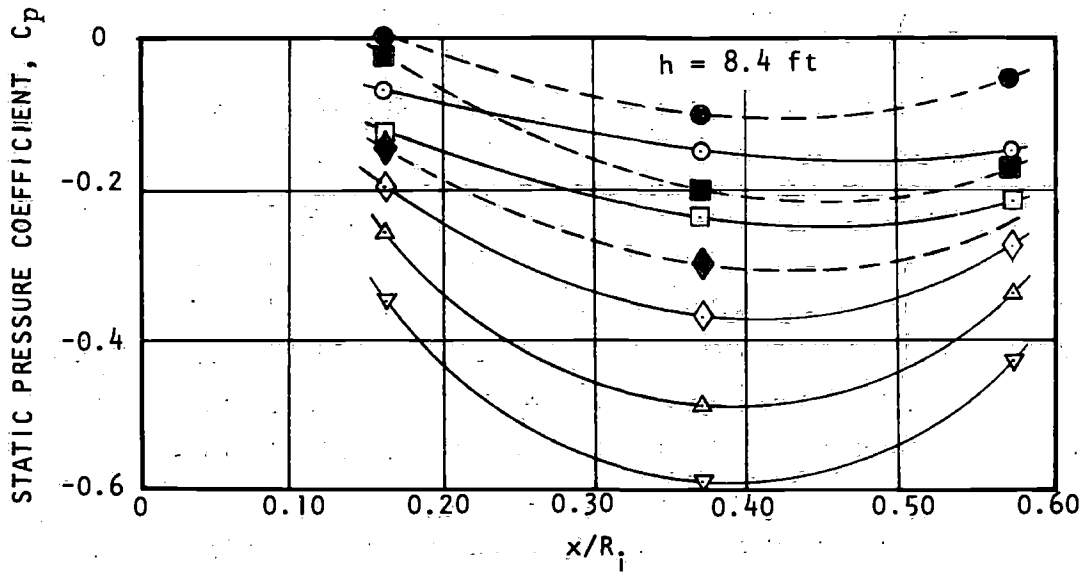


Figure 10 - Effect of Inlet Velocity on the External Nacelle Pressure Distribution at Design Cruise Speed of 50 Knots

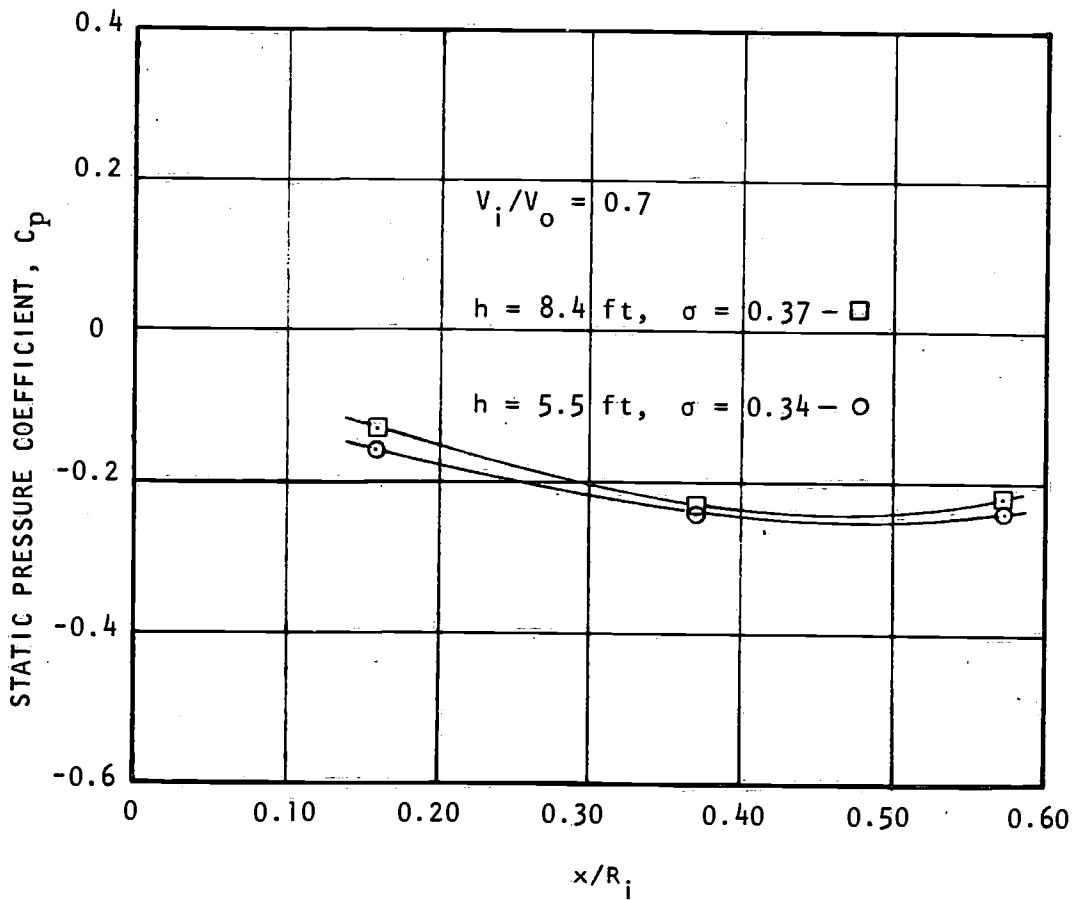


Figure 11 - Effect of Submergence on the External Pressure Distribution at Cruise

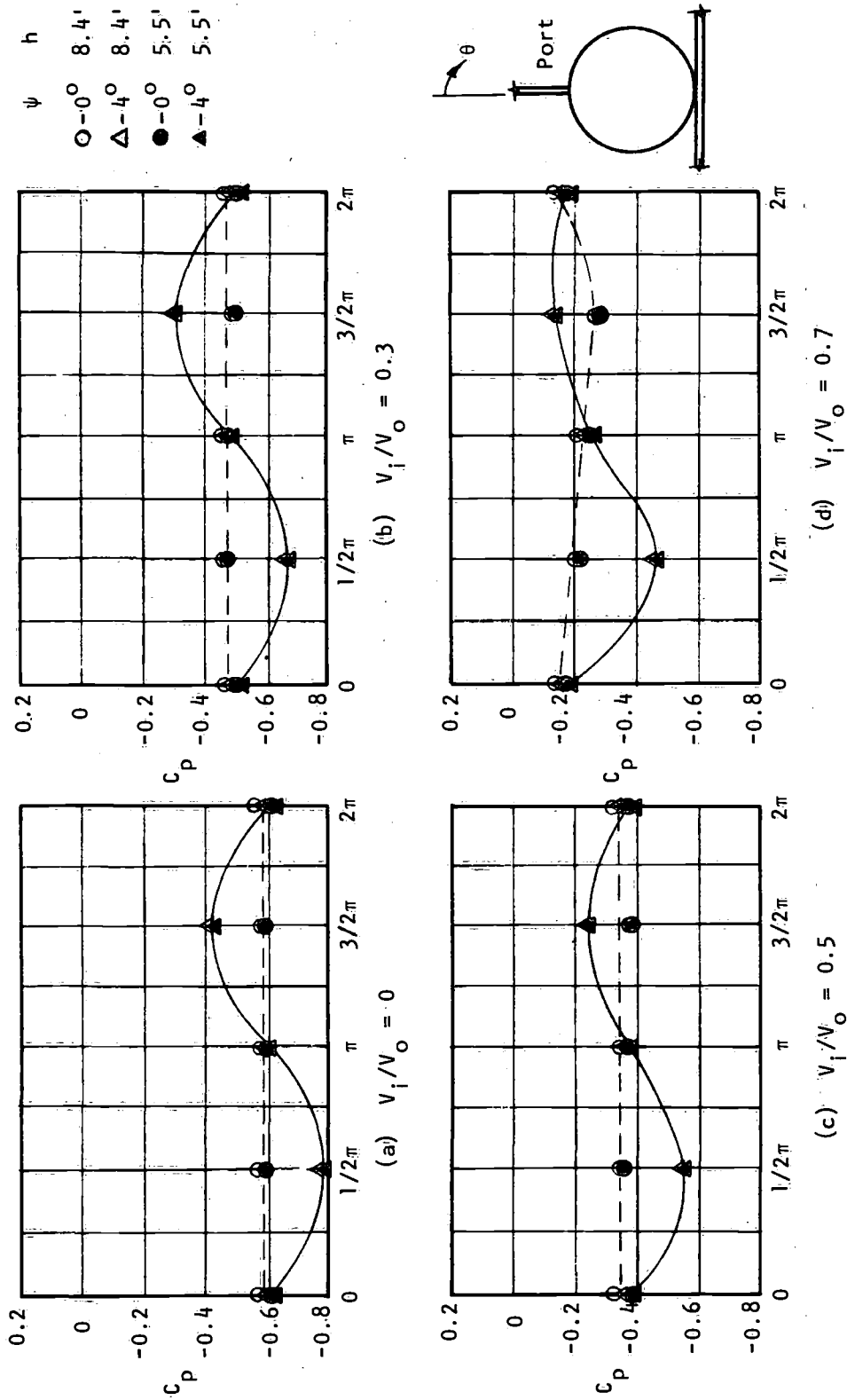


Figure 12 - Effect of Yaw Angle and Submergence on the External Peripheral Pressure Distribution at Cruise

design conditions. Cavitation inception is predicted for $V_i/V_o < 0.5$. At takeoff speed of 30 knots, no cavitation is predicted for $0 < V_i/V_o < 1.2$. This nacelle is considered satisfactory from the cavitation viewpoint.

The total head loss from the inlet to the strut exit (H_D) is plotted against Reynolds number in Figure 13. The total head loss coefficient for the full-scale system may be extrapolated from the measured data as indicated in Figure 13.

CONCLUSIONS

The capability for conducting hydrofoil waterjet propulsion tests at NSRDC has been established. The test rig for this work has been designed and built. The developed experimental procedure and the associated instrumentation have been demonstrated and performed satisfactorily.

The nacelle tested demonstrates satisfactory cavitation inception performance at takeoff and design cruise conditions.

NSRDC measured lift and drag forces compare well with those obtained by Lockheed. However, a comparison of measured pressure coefficients shows considerable discrepancies. The NSRDC data are considered the more reliable since the test facility permits a longer run time at constant speed for collection of pressure data.

RECOMMENDATIONS

To improve the procedure for conducting hydrofoil waterjet propulsion tests, the following are recommended:

1. A potential flow computation or a wind tunnel test (no free surface effect) for predicting the location of the minimum pressure should be made before the experiments at the high-speed basin. The results may be used as a guide to locate the static pressure taps. Three to five taps in the vicinity of the minimum pressure point are sufficient to determine the effect of the free surface on the cavitation inception at the nacelle.

2. A careful calibration of gage assembly together with the flexible rubber joint should be performed. A pressure above 15 psi in the present flexible joint is not recommended.

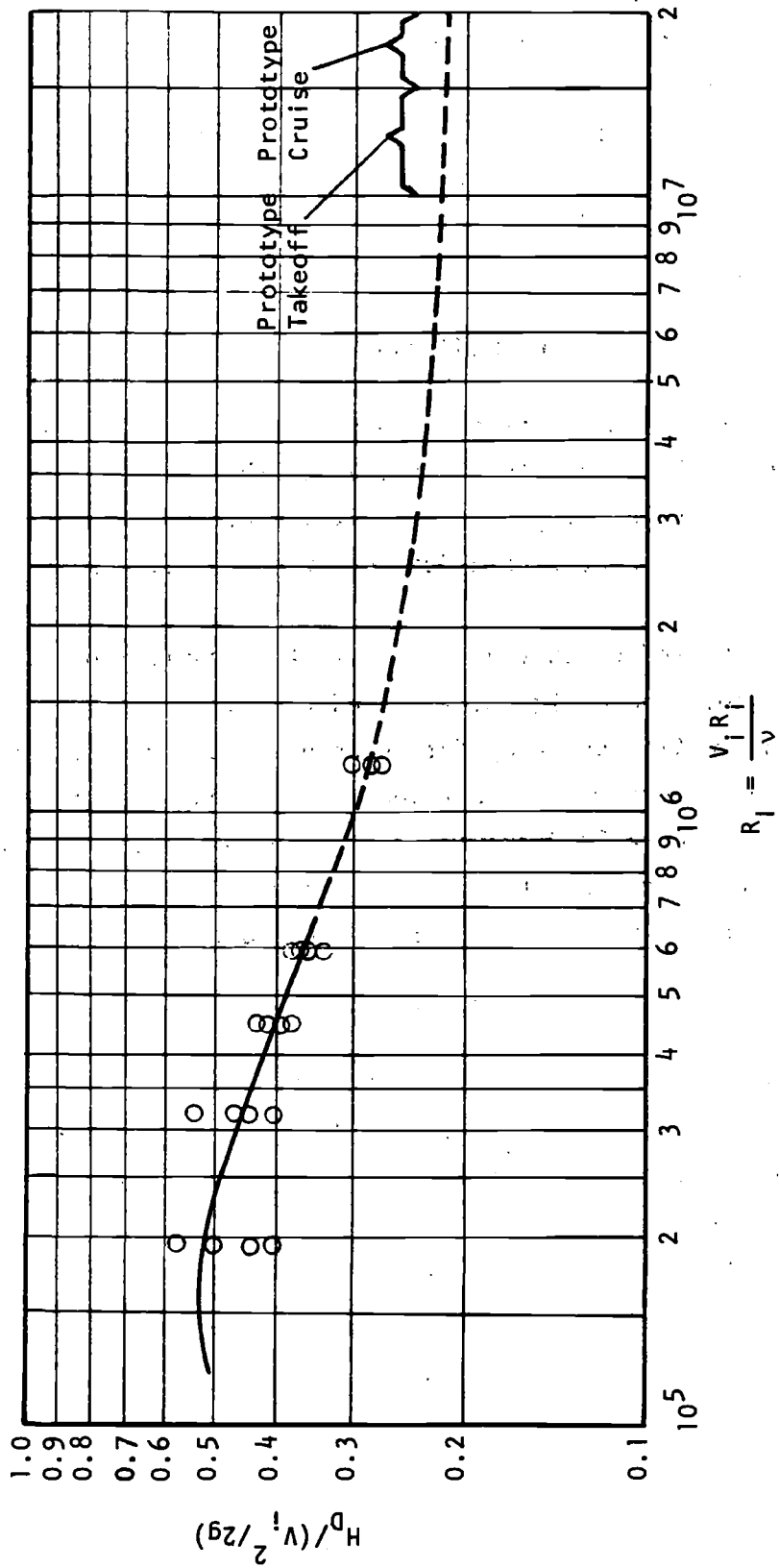


Figure 13 - Head Loss Coefficients from Inlet to Strut Exit

3. A control valve at a proper location of the ducting system should be used to regulate larger ranges of the flow rate through the propulsion system.

4. Force on the deflection elbow may be used to check the flow rate discharged from the nozzle.

REFERENCES

1. Brown, J. and Traksel, J., "Waterjet Propulsion Study," Lockheed California Company, Report LR-17885, Parts 1-5 (1963).

2. Vincent, M. da C., "The Naval Ship Research and Development Center," NSRDC Report 3039 (Jun 1969).

3. Ficken, N.L. and Dobay, G.F., "Experimental Determination of the Forces on Supercavitating Hydrofoils with Internal Ventilation," David Taylor Model Basin Report 1676 (Jan 1963).

4. Rouse, H., "Elementary Mechanics of Fluids," 13th Printing, John Wiley and Sons, Inc., New York (Aug 1960).

5. "Instruments and Apparatus," ASME Paper Test Code, Part 5, Chapter 4 (1959).

INITIAL DISTRIBUTION

| Copies | | Copies | |
|--------|--|--------|--|
| 4 | NAVSHIPS | 1 | CO, USNELC Attn: Lib |
| | 3 SHIPS 2052 | | |
| | 1 SHIPS 033 | 1 | CO & DIR, USNAVCIENGLAB |
| 8 | NAVSEC | 1 | NNS&DD, Engr Tech Dept |
| | 1 SEC 6100 | 1 | USNAVPGSCOL, Monterey |
| | 2 SEC 6110 | | |
| | 1 SEC 6144 | 20 | DDC |
| | 2 SEC 6148 | | |
| 1 | NAVORDSYSOM (ORD 05411) | 2 | NASA Attn: 1 Dr. W.L. Haberman (Code MTX) |
| 3 | NAVAIRSYSOM | 1 | Director of Research (Code RR) |
| | 2 AIR 604 | | |
| | 1 AIR 302 | | |
| 3 | CHONR | 2 | ADMIN, MARAD 1 Attn: Ship Div 1 Attn: Coordinator of Research |
| | 2 Fluid Dyn (Code 438) | | |
| | 1 Sys & Res Gp. (Code 492) | | |
| 1 | CDR, NUWC | 1 | CO, MSTs |
| 1 | CDR, NWC | 1 | BUSTAND, Attn: Lib |
| 1 | CDR, USNOL | 1 | Library of Congress, Wash |
| 1 | DIR, USNRL | 1 | SUPT, USMA Commandant, USCOGARD Attn: Ship Construction Comm |
| 1 | ONR, SAN FRAN | 1 | Commander, U.S. Army Transp Res & Dev, Fort Eustis, Va Attn: Marine Transp Div |
| 1 | CO, ONR, BSN | | |
| 1 | CO, ONR, Pasadena | 1 | Air Force Office of Sci Res, Wash, Attn: Mechanics Div |
| 1 | CO, ONR, Chicago | 1 | W-PAFB, Dayton Attn: Wright Air Dev Div, Aircraft Lab |
| 1 | CO, ONR, London | 2 | Langley Res Center, Langley Station, Hampton, Va Attn: 1 Mr. I.E. Garrick 1 Mr. D.J. Marten |
| 1 | NAVSHIPYD PTSMH | | |
| 1 | NAVSHIPYD BSN | | |
| 1 | NAVSHIPYD BREM | | |
| 1 | NAVSHIPYD PHILA | | |
| 1 | NAVSHIPYD CHASN | | |
| 1 | NAVSHIPYD LBEACH | | |
| 1 | CDR, NWL Attn: Computation & Exterior Ballistics Lab | 1 | DIR, Nat'l Sci Foundation, Wash, Attn: Engr Sci Div |
| 1 | CO, USNROTC & NAVADMINUMIT | 1 | Chief of Res & Dev, Office of Chief of Staff, Dept of the Army, the Pentagon |
| 1 | Supt, USNA | | |
| 1 | CO, USNAVUWRES Attn: Lib | 1 | DIR, WHOI |

Copies

1 NASA, College Park
Attn: Scientific & Techn Info,
Acquisitions Br

1 Commander Gen, Army Eng Res &
Dev Lab, Fort Belvoir, Va
Attn: Technical Documents
Center

1 DIR, ORL, Penn State

1 Head, Dept NAME, MIT

4 CIT
1 Attn: Lib
1 Attn: Prof Acosta
1 Attn: Prof Plesset
1 Attn: Prof Wu

1 DIR, St. Anthony Falls
Hydraulic Lab, Univ of Minn,
Minneapolis

1 Univ of Notre Dame, Dept of
Mech Eng, South Bend

1 DIR, Inst of Hydraulic Res,
Univ of Iowa, Iowa City

1 Univ of Michigan, Dept NAME,
Ann Arbor

1 Webb Inst of Naval Arch,
Glen Cove, 1 Attn: Lib

2 Univ of Calif, Berkeley
1 Attn: Lib
1 Attn: Head, Dept NAVARCH

2 State Univ of Colorado,
Fort Collins, Colorado
1 Attn: Dr. M.L. Albertson
1 Attn: Prof J.E. Germak

1 Cornell Univ, Graduate School
Aeronautical Eng, Ithaca

1 Harvard Univ, Cambridge
Attn: Lib

2 JHU, Baltimore
1 Attn: Dept of Mechanics
1 Attn: Inst of Cooperative
Res

2 State Univ of New York,
Maritime College, Bronx, N.Y.
1 Attn: Engineering Dept
1 Attn: Inst of Math Sci

Copies

1 Princeton Univ, Princeton,
New Jersey, Attn: Lib

1 Stanford Univ, Stanford,
Calif, Attn: Dept of
Civil Eng

1 Univ of Illinois, Dept of
Theoretical & Applied
Mechanics, Urbana

1 JHU, Fenton Kennedy
Document Center, Applied
Physics Lab, Silver Spring

1 Cornell Aeronautical Lab,
Buffalo

2 Davidson Lab, SIT, Hoboken
1 Attn: Director
1 Attn: Dr. Tsakonas

1 Rensselaer Polytechnic Inst,
Dept of Mathematics,
Troy, N.Y.

1 Puget Sound Bridge &
Drydock Co, Seattle

1 Douglas Aircraft Co,
General Applied Sci Lab,
Westbury, L.I., N.Y.

1 ITEK Corp, Vidya Div,
Palo Alto

1 TRG Inc, Melville, N.Y.

1 Therm Inc

1 Lockheed Missiles & Space,
Sunnyvale, Attn: Dept 5701

1 Lockheed Missiles & Space,
Palo Alto, Attn: Tech Info
Center

1 Electric Boat Co,
Gen Dynamics Corp, Groton

1 Robert Taggart Inc,
Fairfax, Va

1 Oceanics

1 Gibbs & Cox

1 George G. Sharp, Inc.

1 Grumman Aircraft Corp.,
Bethpage

Copies

- 1 Hydronautics, Inc.
- 1 Martin Co, Baltimore
- 1 Boeing Aircraft, AMS Div,
Seattle
- 1 United Aircraft, Hamilton
Standard Div, Windsor Locks,
Conn
- 1 AVCO, Lycoming Div, Wash
- 1 Baker Mfg, Evansville
- 2 General Dynamics - Convair Div,
San Diego
 - 1 Attn: Dr. B.R. Parkin
 - 1 Attn: Chief of ASW/Marine Sci
- 1 Curtiss-Wright Corp,
Woodridge, N.J.
- 1 FMC
- 1 President, General Technical
Services Inc, Cleveland
- 1 Dr. S.F. Hoerner, 148 Busted Drive,
Midland Park, N.J.
- 1 RCA, Burlington, Mass
Attention Hydrofoil Projects
- 1 U.S. Rubber Co, Res & Dev Dept,
Wayne, N.J.
- 1 Midwest Research Inst,
Kansas City, Mo
Attn: Lib
- 1 North American Aviation Inc,
Oceans Systems Div,
Downey, Calif
- 1 Aerojet-General Corp, Azusa
- 1 SNAME
- 1 ASNE, Washington
- 1 ASME, Res Comm in Information,
New York
- 1 Inst of Aerospace Sciences, New York
Attn: Lib

UNCLASSIFIED

Security Classification

DOCUMENT CONTROL DATA - R & D

(Security classification of title, body of abstract and indexing annotation must be entered when the overall report is classified)

| | |
|--|--|
| 1. ORIGINATING ACTIVITY (Corporate author) Naval Ship Research and Development Center Washington, D.C. 20007 | 2a. REPORT SECURITY CLASSIFICATION UNCLASSIFIED 2b. GROUP |
|--|--|

3. REPORT TITLE

DEVELOPMENT OF A HYDROFOIL WATERJET PROPULSION SYSTEM TEST FACILITY

4. DESCRIPTIVE NOTES (Type of report and inclusive dates)

5. AUTHOR(S) (First name, middle initial, last name)

Thomas T. Huang and Garnell S. Belt

| | | |
|----------------------------|------------------------------|----------------------|
| 6. REPORT DATE May 1970 | 7a. TOTAL NO. OF PAGES 32 | 7b. NO. OF REFS 5 |
|----------------------------|------------------------------|----------------------|

| | |
|--|--|
| 8a. CONTRACT OR GRANT NO. b. PROJECT NO. S-4606X c. Task 01722 d. | 9a. ORIGINATOR'S REPORT NUMBER(S) 3318 9b. OTHER REPORT NO(S) (Any other numbers that may be assigned this report) |
|--|--|

10. DISTRIBUTION STATEMENT
This document has been approved for public release and sale; its distribution is unlimited.

| | |
|-------------------------|--|
| 11. SUPPLEMENTARY NOTES | 12. SPONSORING MILITARY ACTIVITY Hydrofoil Development Program Office Naval Ship Research and Development Center |
|-------------------------|--|

13. ABSTRACT

The Naval Ship Research and Development Center (NSRDC) has established the capability for conducting hydrofoil waterjet propulsion tests. A test rig was designed and built, utilizing an existing planar-motion mechanism (PMM), for use in the high-speed towing basin. An experimental procedure and associated instrumentation were also developed for these experiments. An experiment using an existing nacelle-strut-foil hydrofoil model was made to demonstrate this capability at the Center.

UNCLASSIFIED

Security Classification

| 14. KEY WORDS | LINK A | | LINK B | | LINK C | |
|--|--------|----|--------|----|--------|----|
| | ROLE | WT | ROLE | WT | ROLE | WT |
| Hydrofoil Waterjet Propulsion <i>Propeller</i> <i>Instrumentation</i> <i>description</i> NSRSC USA | | | | | | |

UNCLASSIFIED

Security Classification